

Electronic, magnetic and optical properties of random Fe-Cr alloys

Kartick Tarafder,¹ Atisdipankar Chakrabarti,² Subhradip Ghosh,³ Biplab Sanyal,⁴ Olle Eriksson,⁴ and Abhijit Mookerjee¹

¹*S.N. Bose National Center for Basic Sciences, JD-III, Salt Lake City, Kolkata 700098, India*

²*R.K. Mission Vivekananda Centenary College, Rahara, Kolkata 700118, India*

³*Department of Physics, Indian Institute of Technology, Guwahati, India*

⁴*Theoretical Magnetism Group, Department of Physics, Uppsala University, SE-75121, Sweden*

(Dated: September 5, 2021)

In this communication we have studied the electronic structure, magnetic and optical properties of bcc $\text{Fe}_x\text{Cr}_{1-x}$ alloys in the ferromagnetic phase. We have used the augmented space recursion technique coupled with tight-binding linearized muffin-tin orbital technique (TB-LMTO-ASR) as well as the coherent-potential approximation based on the Korringa-Kohn-Rostocker method (KKR-CPA). Also the plane wave projector augmented wave (PAW) method has been used with the disorder simulated by the special quasi-random structure method for configuration averaging (SQS). This was to provide a comparison between the different methods in common use for random alloys. Moreover, using the self-consistent potential parameters from TB-LMTO-ASR calculations we obtained the spin resolved optical conductivity using the generalized recursion technique proposed by Müller and Vishwanathan.

PACS numbers: 71.20.Gj, 71.23.-k, 36.40.Cg

I. INTRODUCTION

Multi-layers of magnetic metals have attracted attention because of their possible applications in designing devices. Fe-Cr multi-layers in particular have been studied¹. It has been felt that in order to understand multi-layers, we must first attempt to understand binary inter-metallic compounds as well as random binary alloys : the former, since in the B2 structure they are naturally occurring models of single atomic multi-layers, and the latter, in particular, to give insight into disordering at the multilayer interfaces².

There are ample experimental investigations on this alloy system. These include studies on structural phase stability and phase diagrams³⁻¹¹, spinodal decomposition¹²⁻¹³, structural studies from X-Ray scattering¹⁴⁻¹⁵, inelastic neutron scattering¹⁶⁻¹⁷, Mössbauer¹⁸⁻²², heat capacity²³⁻²⁵, thermopower²⁶, the magnetic phase stability²⁷ and magnetic phases of $\text{Fe}_x\text{Cr}_{1-x}$ alloys²⁸⁻³⁸. They provide a variety of information, e.g. variation of magnetization with band filling³⁹, moment distribution in dilute Fe based alloys⁴⁰, composition dependence of high field susceptibility⁴¹, low-temperature specific heat⁴² and resistivity anomaly⁴³.

Theoretical investigations have been carried out on the phase stability of $\text{Fe}_x\text{Cr}_{1-x}$ alloys⁴⁴⁻⁵¹. There have been several calculations on ordered inter-metallic Fe-Cr in the B2 structure using standard electronic structure methods^{2,52-55}. Studies on Fe-Cr in the σ phase have also been reported⁵⁶.

Magnetism in this alloy has been studied by the spin polarized KKR-CPA method by many authors^{54,57}. Butler *et.al.*⁵⁸ have studied the GMR effect in the concentration range of ($0.5 < x < 0.1$) and antiferro- to ferro-magnetic

transition at the critical concentration of $x = 0.3$. Dederichs *et.al.*⁵⁹ have discussed the Slater-Pauling curves of $\text{Fe}_x\text{Cr}_{1-x}$. Kulikov *et.al.*⁶⁰ have shown that body-centered cubic Fe moments are fairly independent of Cr concentration, while the opposite is true for Cr.

Jiang *et.al.*⁶¹ have studied the local environment effect on the formation enthalpy, magnetic moments, equilibrium lattice parameter and bond lengths using special quasi-random structure (SQS), a concept proposed by Zunger *et.al.*⁶². With a 16-atom SQS super-cell they have shown that even for a lattice-matched system like Fe-Cr the average Cr-Cr, Cr-Fe, Fe-Fe bond lengths are quite different. For magnetic moment calculation they have obtained reliable results in the concentration range of $x > 0.3$. Very recently, Olsson *et.al.*⁶³ have studied the stability of FeCr alloys in the ferromagnetic phase. They argued that the negative mixing enthalpy responsible for this stability has an electronic origin. They also showed that PAW-SQS calculations of mixing enthalpy and magnetic moments were in very good agreement with CPA coupled with the exact-muffin-tin-orbital method.

It is evident from our introductory remarks and the wealth of references given, that the $\text{Fe}_x\text{Cr}_{1-x}$ alloy system has been studied thoroughly both experimentally and theoretically for quite some time now. There can be no justification for one more calculation using one more method at this stage. However, what has not been done so far is a systematic analysis and comparison of the results of the principal successful methodologies. Such a study will give us a clear picture of the comparative strengths and weaknesses of these methods vis-a-vis one another. An extensively experimentally studied alloy, like $\text{Fe}_x\text{Cr}_{1-x}$, is then an excellent choice of a system on which to carry out such a comparative analysis. This

is the basic aim of the work presented here.

We shall identify a few of the first-principles electronic structure methods for disordered alloys which we believe to be the most accurate and make a comparative analysis of results obtained through them for $\text{Fe}_x\text{Cr}_{1-x}$. Different properties like optical response and magnetic transition temperatures have rarely been studied using the same electronic structure methods coupled with different approximations dealing with disorder. This will provide insights into the advantages and drawbacks of these techniques and give us confidence in their use for future studies on different alloy systems.

We have identified three electronic structure methods for disordered substitutional binary alloys : the Korringa-Kohn-Rostocker based mean field coherent potential approximation (KKR-CPA)⁶⁶, the projector augmented wave based super-cell calculations on special quasi-random structures (PAW-SQS)⁶² and the tight-binding linear muffin-tin orbitals based augmented space recursion (TB-LMTO-ASR)⁶⁷. The KKR and its linear version, LMTO, are among the accurate techniques in use for the study of random substitutional alloys, where the disorder induced scattering is *local*. Of course, LMTO being a linearized approximation to the KKR, is expected to be less accurate. However, if the energy window around the linearization energy nodes is not too large, the LMTO estimates energies with tolerances of around 5-10 mRy. Unless we are interested in estimating energy differences smaller than this quantity or over large energy windows, the LMTO is good enough and has the great advantage that its secular equation is an eigenvalue problem rather than the more complicated functional equation of the KKR. In PAW calculations, we have the advantage of a full potential without any shape approximation. It has already been shown that electronic structures of alloys are quite well described with the SQS method⁶⁸. We shall use all three of these methods and compare and contrast the corresponding results.

Methods to deal with disorder fall into three categories. In the first category belongs the single-site mean-field CPA. This approximation has been eminently successful in dealing with a variety of disordered systems. However, whenever there is either strong disorder fluctuation scattering, as in dilute, split-band alloys or when local environment effects like short-ranged ordering, clustering and segregation, or local lattice distortions due to size mismatch of the constituent atoms become important, the single-site based CPA becomes inadequate.

In the second category belong the generalizations of the CPA, of which, the augmented space based methods : the itinerant CPA⁶⁹ (ICPA) and the augmented space recursion (ASR)⁷⁰, are foremost. They not only retain the necessary analytic (Herglotz⁷¹) properties of the averaged Green function, as the CPA does, but also properly incorporate local environment effects.

In the third category belong the super-cell based calculations. Zunger⁶² suggested that if we construct a super-

cell and populate its lattice points randomly by the constituents so as to mimic the concentration correlations in the random alloy, a single calculation with this super-lattice should approximate the configuration average in the infinite random system. The SQS approach has been used to incorporate short-ranged order and local lattice distortions in alloy systems. Certainly, in the limit of a very large super-cell this statement is the *theorem of spatial ergodicity*. This theorem provides the explanation of why a single experiment on global property of a bulk material most often produces the configuration averaged result, provided the property we are looking at is *self-averaging*. How far this approach is accurate with a small cluster of, say, 16 atoms, is a priori uncertain. We shall use the SQS method for averaging as well and compare this with our mean-field and ASR results.

Before we proceed further, we should note that all the three methods, described earlier, to deal with disorder are essentially real space approaches. The disorder is substitutional and *at a site*. There is a fourth technique recently introduced based on a reciprocal-space renormalization method : the non-local CPA. The basic technique was introduced by Jarrel and Krishnamurthy⁶⁴ and applied to CuZn alloys by Rowlands *et.al.*⁶⁵. The method is capable of taking into account environmental effects and short-ranged ordering. As expertise in this method was not available with us we could not include it in this work. Once work on FeCr is available using this technique, it would be interesting to compare the results with what we project here.

A systematic comparison between these calculations will allow us to ascertain, for example, whether the CPA is indeed inadequate in some situations and how far the augmented space based techniques improve matters. We shall extend the TB-LMTO-ASR method also to study the optical response of $\text{Fe}_x\text{Cr}_{1-x}$ alloys. We are not aware of experimental studies of optical conductivity on this alloy system and our preliminary results will provide incentive for further experimental studies.

Ghosh *et.al.*⁷² have earlier studied the same alloy system. Their approach was different from our ASR work here. In the earlier work the authors used the charge neutral sphere approximation proposed by Kudrnovský *et.al.*⁷³ to bypass any Madelung contribution to the total energy. This procedure is both cumbersome and, as we discussed in an earlier paper⁷⁴, such volume conserving charge neutral spheres may not necessarily be found. Our present work uses the ideas of Ruban and Skriver⁷⁵ to estimate the Madelung energy of charged atomic spheres during the LDA self-consistency loops. This earlier work did not observe any sign of the experimentally observed reversal of the Cr projected magnetic moment as a function of Fe concentration.

II. ELECTRONIC AND MAGNETIC STRUCTURE OF $\text{Fe}_x\text{Cr}_{1-x}$ ALLOYS

A. Density of States

Fig. 1 compares the density of states for the spin-up and spin-down states for $\text{Fe}_x\text{Cr}_{1-x}$ across the composition range $0.3 \leq x \leq 0.95$ in which the solid solution in the bcc lattice and the ferromagnetic state is stable at low temperatures. Both the KKR-CPA and TB-LMTO-ASR were carried out within the LSDA self-consistency with the same Ceperley-Alder exchange correlation functional with Perdew-Zunger parametrization. The densities of states for both the approaches show remarkable similarities except in the low Cr compositions. This is expected. The d -band centers of Fe and Cr are well separated, in such a situation, it has been known that for the dilute concentrations the CPA is not accurate. Originally, it was to reproduce this regime of parameters, i.e. dilute limit in the *split band* case that the generalizations to the CPA were proposed. The effect here is, however, small as compared with our earlier analysis of $\text{Cu}_x\text{Zn}_{1-x}$ ⁷⁶.

Of course there are differences in detail. The KKR-CPA is a reciprocal space based approach while the TB-LMTO-ASR is a real space based one and the approximations in the two cases are different. The KKR-CPA is based on a single-site mean field and relevant Brillouin zone integration involves techniques like the tetrahedron integration. The TB-LMTO-ASR expands the configuration averaged Green function as a continued fraction and the main approximation involves calculation of its asymptotic “terminator”. As compared with an earlier work on $\text{Cu}_x\text{Zn}_{1-x}$ ⁷⁶, where the ASR showed considerable improvement over the CPA, in this particular alloy system the differences are much less prominent, except in the very dilute limit. This is an important observation, and we should be careful in making general and strong statements about the efficiency of one method over the other. The results are strongly system dependent.

For the PW-SQS, we have compared the density at only the 50-50 concentration with TB-LMTO-ASR. This is shown in Fig. 2. This calculation has been done with the plane wave PAW method implemented in the VASP code⁷⁷. 400 eV was considered as the cut-off energy for the basis set. The SQS does simulate disorder, nevertheless, being a super-cell technique, it satisfies Bloch’s Theorem. Therefore, the complex self-energy which arises due to disorder scattering in the ASR is per se absent in SQS calculations. This “life-time” effect smoothens the structures in the ASR density of states and gives them larger widths as compared to the SQS. Therefore, to compare the SQS density of states with the TB-LMTO-ASR or KKR-CPA we have to convolute it with a small Gaussian broadening.

Haydock⁷⁸, in his critique of the recursion method, argued that the density of states is perhaps not the best property to compare between different approximations,

because it is unstable to small perturbations. Thouless⁷⁹ has argued that the spectral density arising out of extended states in a disordered system is extremely sensitive to small perturbations. Minor differences in approximations lead to relatively large changes in the spectral density. Haydock suggested that it would be more proper to compare integrated functions like $M(E) = \int_{-\infty}^E dE' f(E') n(E')$ where $f(E')$ is a well-behaved function of E' . Examples are the integrated density of states, the Fermi and band energies and the various energy moments of the density of states. In fact, most physical properties are integrated functions of this kind.

The Fig. 2 (bottom) shows the first three moments of the density of states. The moments have been calculated with normalized densities of states, so that the integrated density of states (which is the zero-th energy moment of the density of states) is 1 at $E=E_F$ for all the three approximations. The moments match well throughout the energy range up to the Fermi energy with the relative deviations being no more than 10% throughout the energy range of interest. Simply from the density of states there is little to choose between the different methods.

B. Short-Ranged Ordering.

The phase diagram of Fe-Cr is simple at high temperatures⁸⁰ and a complete range of bcc solid solutions exists from 1093K to the solidus. Alloys quenched from these temperatures retain their bcc structure. However, the alloys are not homogeneously disordered. Neutron scattering experiments³⁹ indicate that short-ranged clustering exists in these quenched alloys leading to a miscibility gap at temperatures lower than 793K. The single site CPA cannot deal with short-ranged order as the latter explicitly involves independent scattering from more than one site. Attempts to develop generalizations of the coherent potential approximation (CPA) including effects of short-ranged order (SRO) have been many, spread over the last several decades. Many of them fail the analyticity test. Mookerjee and Prasad⁸¹ generalized the augmented space theorem to include correlated disorder. However, since they then went on to apply it in the cluster CPA approximation, they could not go beyond the two-site cluster and that too only in model Hamiltonians. The breakthrough came with the augmented space recursion (ASR) approach proposed by Saha *et.al.*^{82–83}. The method was a departure from the mean-field approaches which always began by embedding a cluster in an effective medium which was then obtained self-consistently. As discussed earlier, here the Green function was expanded in a continued fraction whose asymptotic part was obtained from its initial steps through an ingenious *termination* procedure⁷⁸. In this method the effect at a site of quite a large environment around it could be taken into account depending how far one went down the continued fraction before *termination*.

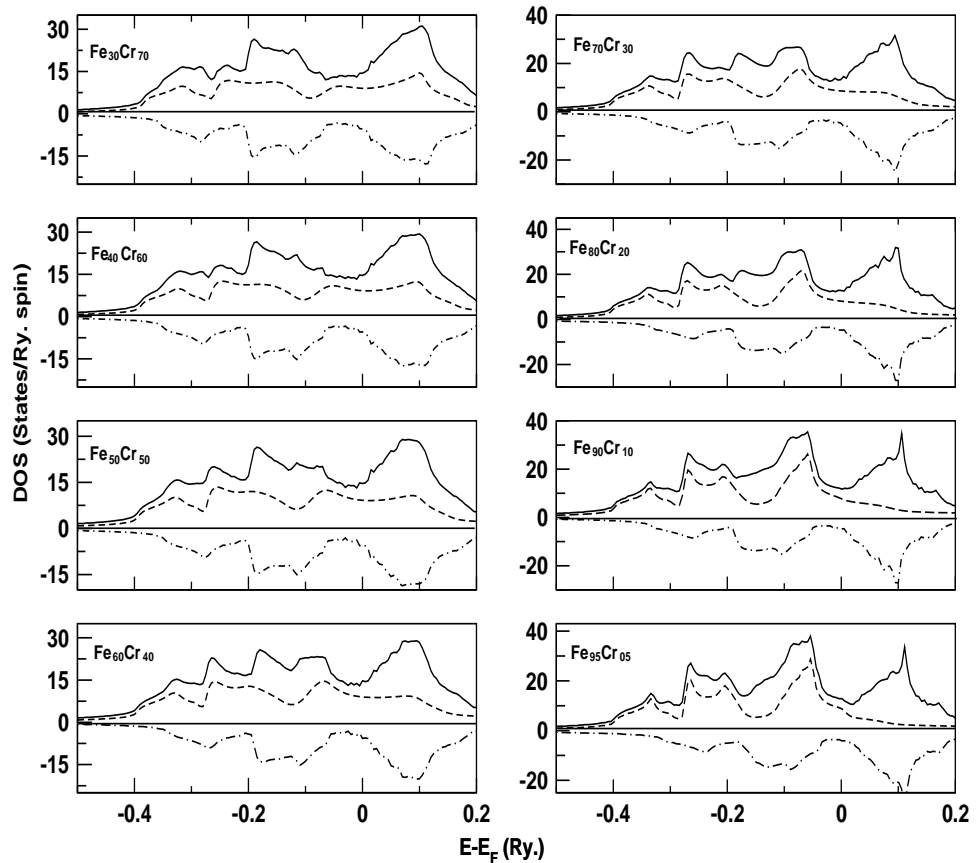
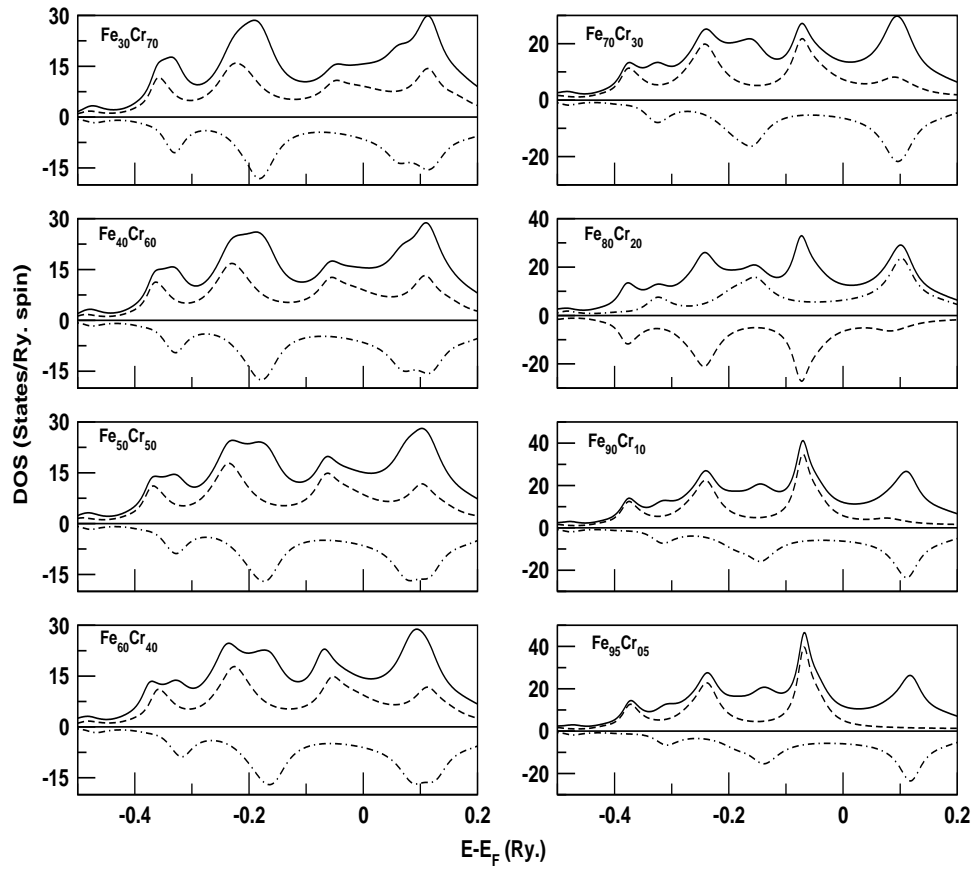


FIG. 1: Densities of states for the spin-up states (upright curves in dashed lines) spin-down states (inverted curves with dashed lines) and total density of states (full lines) for $\text{Fe}_x\text{Cr}_{1-x}$ for various compositions in the ferromagnetic, bcc, disordered phase.

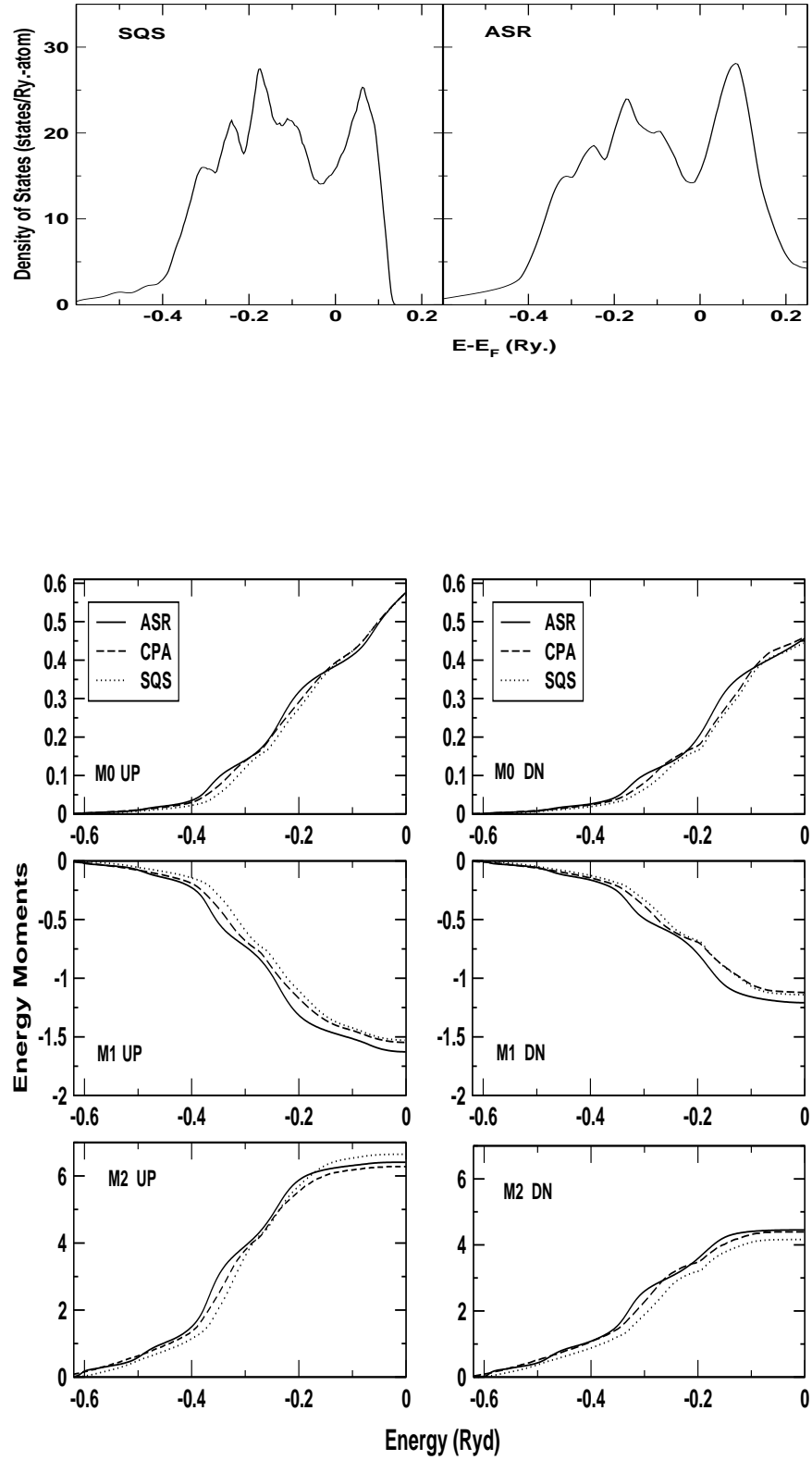


FIG. 2: (top) Densities of states for $\text{Fe}_{50}\text{Cr}_{50}$ obtained from the TB-LMTO-ASR and PAW-SQS methods. (bottom) The first three energy Moments of the density of states (M0, M1 and M2) are shown for the TB-LMTO-ASR, KKR-CPA and PAW-SQS, for up spin (UP) and down spin (DN).

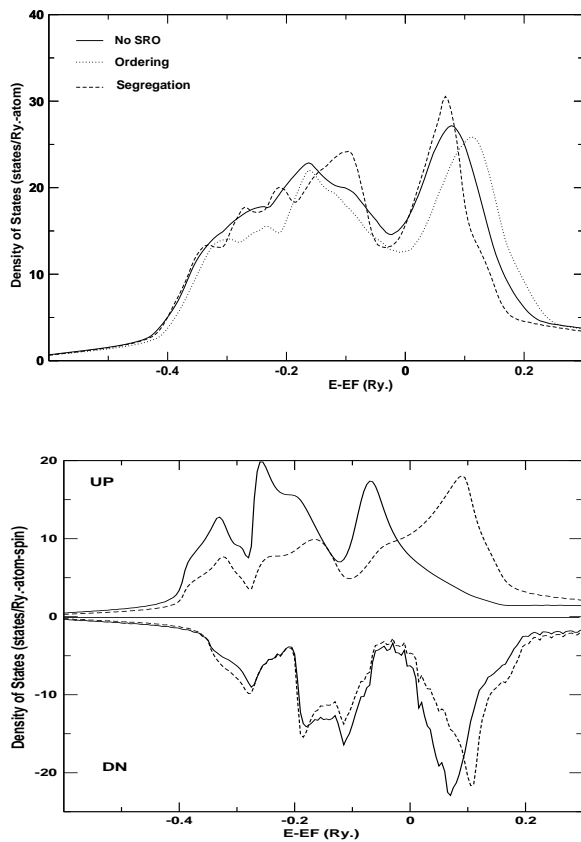


FIG. 3: (top) Density of States for $\text{Fe}_{50}\text{Cr}_{50}$ for (full line) $\alpha=0$ (dotted line) $\alpha=-1$ (dashed line) $\alpha=1$. (bottom) Component and spin projected density of states for $\text{Fe}_{50}\text{Cr}_{50}$ for $\alpha=0$. Fe is shown in full lines and Cr in dashed lines. Upright curves are

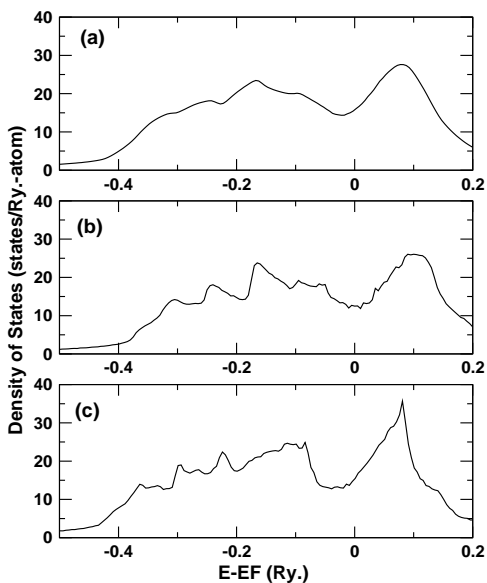


FIG. 4: (top) Density of States for disordered $\text{Fe}_{50}\text{Cr}_{50}$, (middle) Density of States for L12 ordered $\text{Fe}_{50}\text{Cr}_{50}$, (bottom) Density of States for pure Fe and Cr summed up.

The technique was made fully LDA-self-consistent within the TB-LMTO approach⁷⁰ and several applications have been carried out to include short-ranged order in different alloy systems⁷⁴. Details of the formalism has been described in detail in an earlier paper⁷⁶. Here we shall apply it to the case of 50-50 FeCr alloys.

We have carried out the TB-LMTO-ASR calculations on FeCr including short-ranged ordering described by the nearest-neighbour Warren-Cowley parameter α ($-1 \leq \alpha \leq 1$). The Fe and Cr potentials are self-consistently obtained via the LSDA self-consistency loop. All reciprocal space integrals are done by using the generalized tetrahedron integration for disordered systems introduced by us earlier⁸⁴.

To discuss the effect of SRO, leading, on one hand, to ordering ($\alpha < 0$) and segregation on the other ($\alpha > 0$), let us look at Figs. (3) -(4). The component projected density of states with the completely disordered alloy (Fig. 3, bottom) shows rather interestingly that for the down-spin electrons the positions of the centers of the d -bands of Fe and Cr are almost degenerate and strongly hybridize. However, the d -bands of the up-spin electrons are separated in energy. FeCr is then a partially split-band alloy. This implies that for the up-spin electrons the “electrons travel more easily between Fe or between Cr sites than between unlike ones”⁶⁵. So when the alloy orders and unlike sites sit next to each other, the overlap integral between the unlike sites is lower, and for up-spin density of states narrow. For the down-spin bands this effect is not present.

Fig (3) (dashed curve) shows the density of states with $\alpha = 1$. Positive α indicates a clustering or segregating tendency. Comparing with Fig. (4,c), which is a direct sum of the density of states of Fe and Cr, we note that, with clustering, the density of states begins to show the structures seen in the pure metals. For $\alpha = 1$ there is still residual long-ranged disorder. This causes smoothening of the bands with respect to the pure materials. For segregation we notice a shift in the Fe and Cr based structures in the density of states. Again, there is greater smoothening of the density of states structures when the disorder is perfect Fig (3) (full lines). This is due to enhanced disorder scattering leading to larger self-energies. Fig. (3) (dotted curve) shows the density of states with $\alpha = -1$ which indicates nearest neighbour ordering. On the fcc lattice at 50-50 composition we expect this ordering to favor a L12 structure. We can compare with the density of states for the L12 structure shown in Fig. (4). There is a upward shift of the Cr based feature and, as expected, there is less smoothening than the completely disordered case. We have to realize that as we have taken only the nearest neighbour short-ranged order, $\alpha = -1$ does not imply perfect long-ranged ordering.

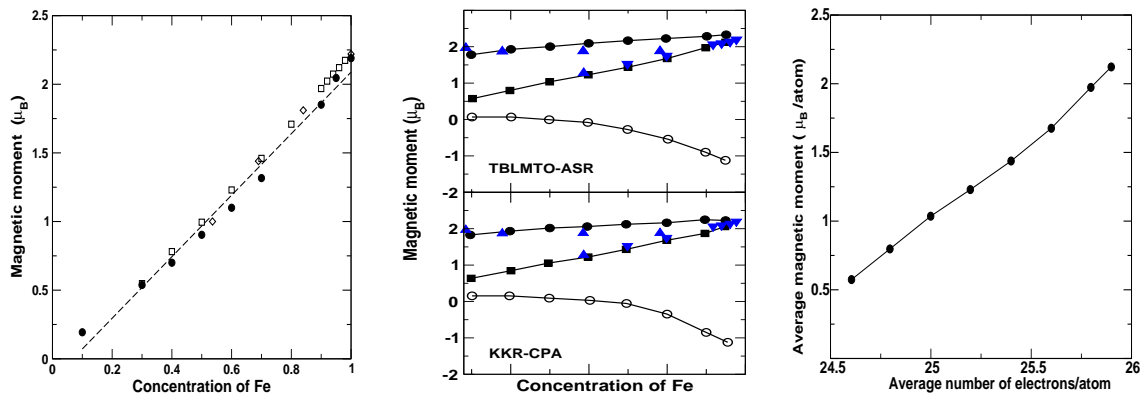


FIG. 5: (left) Compendium of experimental data on the averaged magnetic moment as a function of composition. (middle) Local magnetic moments on Fe (filled circles) and Cr (open circles) and the the average magnetic moment in the alloy (closed squares) for different concentrations of Fe using TB-LMTO-ASR (top panel) and using KKR-CPA (bottom panel). The available experimental data are shown as triangles (bottom) Variation of average magnetic moment with the average number of electrons using TB-LMTO-ASR.

C. Magnetic moments

Experimental work on magnetism in $\text{Fe}_x\text{Cr}_{1-x}$ alloys has a long history. The very earliest works with $\text{Fe}_x\text{Cr}_{1-x}$ are that of Fallot⁸⁵ in 1936 on the variation of the averaged magnetic moment with composition and Shull and Wilkinson⁴⁰ on the neutron-scattering study of Fe-rich $\text{Fe}_x\text{Cr}_{1-x}$ in 1955. Among other properties these studies gave estimates of both the averaged magnetic moments and atom-projected local magnetic moments in this alloy system. Matthews and Morton²⁷ studied FeCr and suggested co-existence of ferro and antiferro-magnetism in the alloy, an idea which was not taken up subsequently. Bulk magnetization measurements were carried out by Aldred³⁹ in 1976. The author also examined theoretical explanations for the averaged magnetic moments in the alloy system and concluded that empirical tight-binding CPA estimates of Hasegawa and Kannamori⁸⁶ and Froliani *et.al.*⁸⁷ gave adequate description of his experimental data. A series of theoretical approaches using different electronic structure methods and usually the CPA followed : notable among these were the works of Moroni and Jarlborg⁵⁴, Singh⁵⁵, Moriatis *et.al.*⁵⁷ and Qiu² whose “fixed moment” method yielded a rather large local moment on Cr compared to the general consensus. Finally, Cieřlak *et.al.*⁴¹ gathered together results for both the Curie temperature and the averaged magnetic moment from resistivity minima⁴³, specific heat anomaly⁴² and elastic measurements⁸⁸. A compendium of the acceptable experimental results on the averaged magnetic moments for different compositions is shown in Fig. (5, top left). Results from different experiments are shown by different symbols. The TB-LMTO-ASR theoretical results which fit the curve $m(x) = 2.44x - 0.244$ is

shown by the dashed curve. The KKR-CPA prediction for the total magnetic moment per atom is almost the same. The theoretical predictions from both the methods agree very well with the experimental results.

Figure 5 (top middle and right) shows the variation of the local and average magnetic moment as a function of Fe concentration of the alloy studied. The results are in good agreement with the few experimental observations available. It shows that the local Fe moment with increasing Fe concentration remains almost constant over the entire concentration range while the Cr moment changes its sign ($x > 0.4$) from low positive value to very high negative value. Earlier studies have also observed similar behavior. The KKR-CPA and TB-LMTO-ASR are in good agreement for the Fe local magnetic moment, while the agreement is less close for the local moment on Cr. Unfortunately, there are no experimental data on the local moment on Cr. This is in contrast to the much better reproduction by the TB-LMTO-ASR of the local moment on Ni in Ni-based alloys, as compared to the CPA. This is because the fragile moment of Ni is dependent strongly on its immediate neighbourhood, which cannot be adequately described by the single-site CPA⁸⁹. The moment on Cr is less dependent on the configuration of its immediate neighbourhood and the CPA here is not a bad description.

These observations can be explained with the help of inter and intra atomic charge transfer effects. This has been shown in Fig.(6). We notice that, for the entire concentration range, Fe gains electronic charge from Cr. We observe that, for the alloy composition $x = 0.3$, Fe gains 0.213 electrons as compared to pure Fe. But the spin up band in Fe in the alloy loses 0.126 electrons, whereas the minority band gains 0.34 electrons, leading to a over-

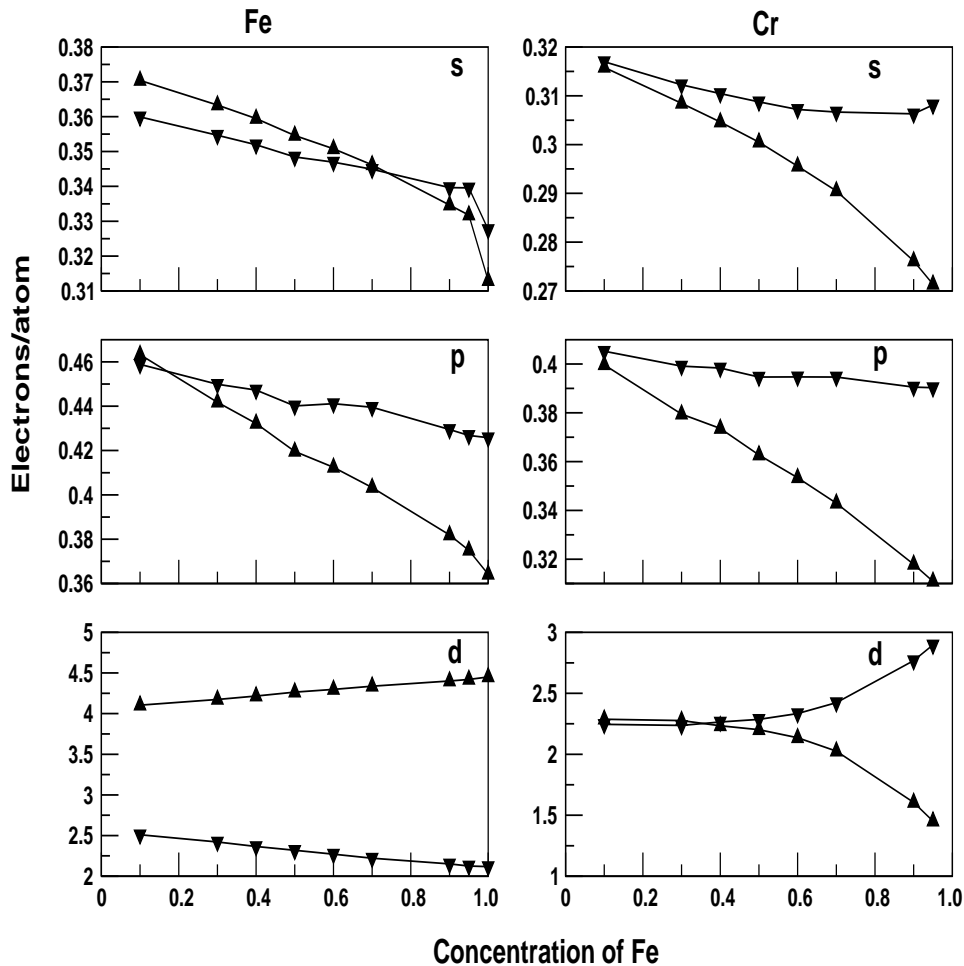


FIG. 6: The orbital resolved changes in the Fe and Cr atomic spheres in $\text{Fe}_x\text{Cr}_{1-x}$ alloys

all reduction in the magnetic moment. A closer study reveals that among the different orbitals in the spin-up states, the s and p orbitals gain charge while the d orbital loses some. On the other hand for the spin-down states all the three orbitals s, p and d gain charge. For the Cr projected site the charge lost or gained is different for different orbitals leading to a small but finite magnetic moment. For the spin-up states the s and d orbitals gain and the p orbital loses charge, while for spin-down states only the s orbital gain and the p and d orbitals lose charge.

For $x = 0.5$ where the Cr projected magnetic moment changes its sign, we observe that the d -up state has more charge than the d -down but the p and s -down states have more charge than their spin-up counterparts. Due to this the overall magnetic moment on a Cr projected site reverses its sign. But for higher concentrations of Fe it is the charges in the d orbitals which decide the magnetic moment of Cr. This interesting interplay between inter

and intra atomic charge transfer has been captured by our analysis.

From Fig. 1 we see that the Fermi energy is pinned to the minimum of the minority spin density of states. But for $x > 0.5$ the majority spin density of states is entirely filled. It shows that with increasing Fe concentration the additional electrons are added mainly to the spin-up d band. As we scan through the concentration range the Cr spin-up density of states shows major ($x > 0.7$) variation. This is understandable as we see that initially, for low x compositions, Cr d -up orbitals tend to acquire more charge than d -down ones, but for $x > 0.5$ compositions the reverse phenomenon is observed. In our calculation this is the critical concentration at which Cr projected magnetic moment reverses its sign.

Figure 5 (bottom panel) shows the variation of average magnetic moment against the average number of electrons. This is the Slater-Pauling curve and it shows a almost a linear variation up to $x = 0.8$, above which the

Cr moment changes very rapidly to larger negative value. This observation is in accordance with earlier studies.

III. OPTICAL CONDUCTIVITY

In an earlier communication⁹² we had developed a completely self-consistent TB-LMTO-ASR based method to study the optical conductivity of alloys using a recursive procedure suggested by Viswanathan and Muller⁹³. Our starting point is the Kubo formula :

$$\begin{aligned} & \ll \chi^{\mu\nu}(t-t') \gg \\ &= \frac{i}{\hbar} \Theta(t-t') \langle \{\emptyset\} \otimes \phi | \tilde{\mathbf{j}}^\mu(t) \tilde{\mathbf{j}}^\nu(t') | \phi \otimes \{\emptyset\} \rangle \end{aligned}$$

$\tilde{\mathbf{j}}^\mu$ is the current operator and Θ is the Heaviside step function. For disordered systems, the Hamiltonian and current operators are constructed in the full configuration space and the Augmented Space theorem tells us that a specific matrix element in this space is the configuration average⁹⁴. If the underlying lattice has cubic symmetry, $\chi^{\mu\nu} = \chi \delta_{\mu\nu}$. The fluctuation dissipation theorem relates the imaginary part of the Laplace transform of the generalized susceptibility to the Laplace transform of a correlation function given by

$$\ll S(\omega) \gg = \int_0^\infty dt \exp\{i(\omega+i\delta)t\} \ll \text{Tr} \left(\tilde{\mathbf{j}}^\mu(t) \tilde{\mathbf{j}}^\mu(0) \right) \gg \quad (1)$$

as

$$\ll \chi''(\omega) \gg = (1/2\hbar) (1 - \exp\{-\beta\hbar\omega\}) \ll S(\omega) \gg$$

We, therefore, have to calculate the configuration average of the correlation function,

$$\ll S(t) \gg = \langle \{\emptyset\} \otimes \phi | \mathbf{j}(t) \mathbf{j}(0) | \phi \otimes \{\emptyset\} \rangle$$

for a given Hamiltonian $i\tilde{\mathbf{H}}$. We determine the correlation directly via the recursion method suggested by Viswanath and Müller. In order to simplify the expressions for the dynamical quantities as produced by the Hamiltonian, we consider henceforth the modified Hamiltonian $\tilde{\mathbf{H}} = \tilde{\mathbf{H}} - E_0 \tilde{\mathbf{I}}$, whose band energy is shifted to zero. If we start from the bra :

$$\langle \psi(t) | = \langle \phi \otimes \{\emptyset\} | \tilde{\mathbf{j}}(t)$$

Its time evolution is governed by the Schrödinger equation

$$-i \frac{d}{dt} \left\{ \langle \psi(t) | \right\} = \langle \psi(t) | \tilde{\mathbf{H}} \quad (2)$$

We now generate an orthogonal basis $\{\langle f_k | \}$ for representation of equation (2) in the following way .

(i) We begin with initial conditions :

$$\langle f_{-1} | = 0 \quad ; \quad \langle f_0 | = \langle \phi \otimes \{\emptyset\} | \mathbf{j}(0)$$

(ii) We now generate the new basis members by a three term recurrence relationship :

$$\langle f_{k+1} | = \langle f_k | \tilde{\mathbf{H}} - \langle f_k | \alpha_k - \langle f_{k-1} | \beta_k^2 \quad k = 0, 1, 2 \dots$$

where,

$$\alpha_k = \frac{\langle f_k | \tilde{\mathbf{H}} | f_k \rangle}{\langle f_k | f_k \rangle} \quad \beta_k^2 = \frac{\langle f_k | f_k \rangle}{\langle f_{k-1} | f_{k-1} \rangle}$$

We now expand the bra $\langle \psi(t) |$ in this orthogonal basis :

$$\langle \psi(t) | = \sum_{k=0}^{\infty} \langle f_k | D_k(t)$$

Substituting and using orthogonality of the basis, we get :

$$-i \dot{D}_k(t) = D_{k-1}(t) + \alpha_k D_k(t) + \beta_{k+1}^2 D_{k+1}(t) \quad (3)$$

with $D_{-1}(t) = 0$ and $D_k(0) = \delta_{k,0}$. We now show that the pair of sequences generated by us, namely, $\{\alpha_k\}$ and $\{\beta_k^2\}$ are enough for us to generate the correlation function. We note first that :

$$D_0(t) = \langle \psi(t) | f_0 \rangle = S(t)$$

Let us define the Laplace transform :

$$d_k(z) = \int_0^\infty dt \exp(-izt) D_k(t)$$

Putting this back in equation(3) we get :

$$(z - \alpha_k) d_k(z) - i\delta_{k,0} = d_{k-1}(z) + \beta_{k+1}^2 d_{k+1}(z)$$

k=0,1,2 ...

This set of equations can be solved for $d_0(z)$ as a continued fraction representation :

$$d_0(z) = \frac{i}{z - \alpha_0 - \frac{\beta_1^2}{z - \alpha_1 - \frac{\beta_2^2}{z - \alpha_2 - \dots}}} \quad (4)$$

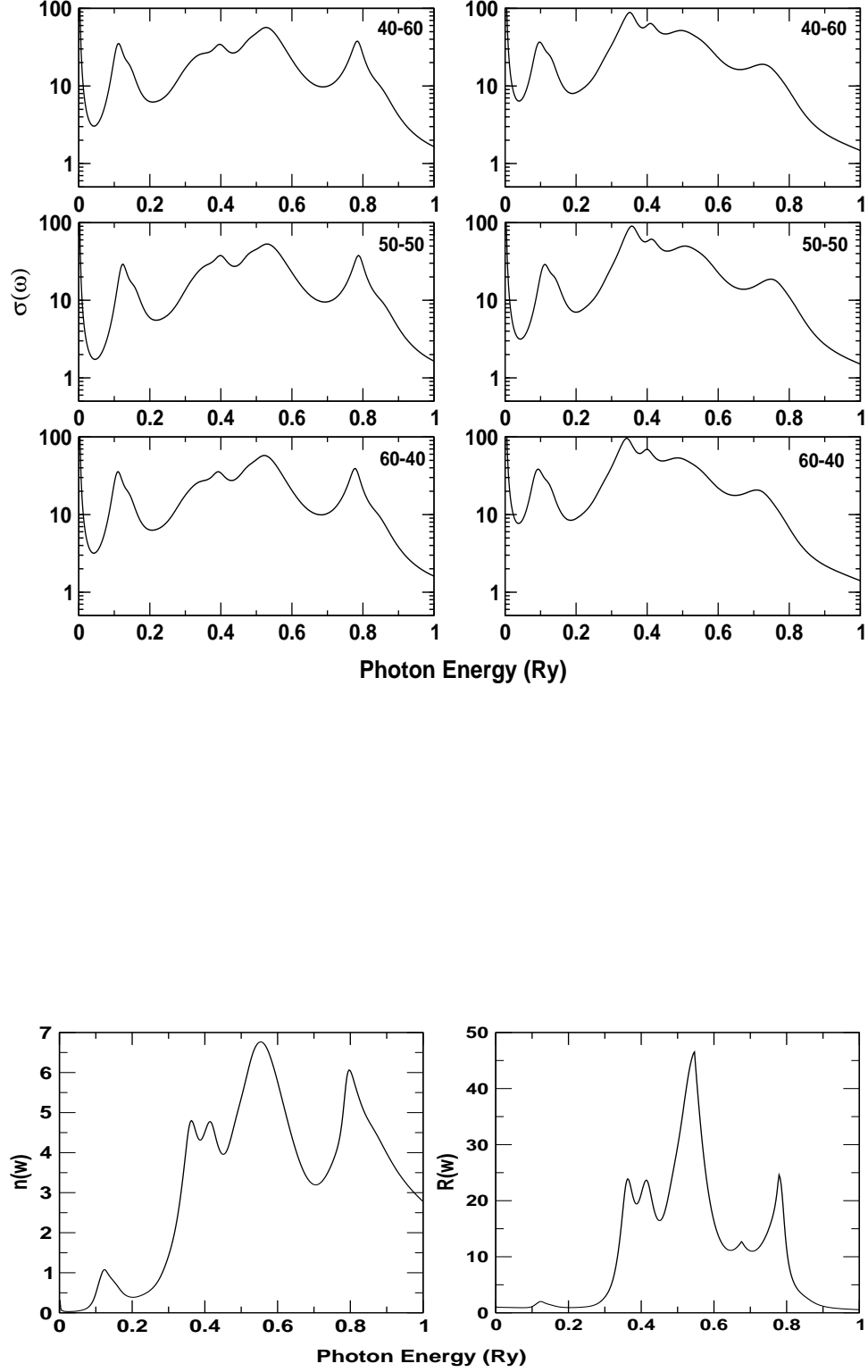


FIG. 7: (top) Optical conductivity for different compositions of the FeCr alloy. Left panels are for the down-spin contributions while the right panels are for the up-spin contributions, (bottom) Left panel shows the refractive index $n(\omega)$ and the right panel shows the reflectivity $R(\omega)$ for the 50-50 alloy

The structure function, which is the Laplace transform of the correlation function can then be obtained from the above :

$$\ll S(\omega) \gg = \lim_{\delta \rightarrow 0} 2 \Re e d_0(\omega + i\delta)$$

The optical conductivity is then given by :

$$\sigma(\omega) = \frac{\ll S(\omega) \gg}{\omega}$$

The imaginary part of the complex dielectric function $\epsilon(\omega)$ is

$$\epsilon_2(\omega) = \frac{4\pi\sigma(\omega)}{\omega}$$

The real part $\epsilon_1(\omega)$ is related to the imaginary part by a Kramer-Krönig relationship.

The refractive index is given by :

$$n(\omega) = \Re e \sqrt{\epsilon(\omega)}$$

Finally, the reflectivity is defined as :

$$R(\omega) = \left| \frac{\sqrt{\epsilon(\omega)} - 1}{\sqrt{\epsilon(\omega)} + 1} \right|^2$$

Figure 7 (top, left panel) shows the variation of the optical conductivity for three different compositions of the FeCr alloy. For low photon energies (≤ 0.05 - 0.06 Ry.) the behaviour is Drude like $\sim \omega^{-2}$. If we have a look at the component and spin-projected density of states (Fig. 3 (bottom)), we note that for these energies the transitions from below the Fermi energy are almost entirely due to $s - p$ like states. Around 0.05 - 0.06 Ry transitions begin from d -up like states coming from Cr which gives the characteristic peaked structures in the density of states. Now the optical conductivity picks up and subsequent transitions reflect the structures in the joint densities of states of the alloy. It is clear that this non-Drude behaviour begins for slightly larger energies for the down-states, so the Drude decay for the down-spin contribution (top left panel in Fig 7) is more than that for the up-spin contribution (top right panel in Fig. 7).

The bottom panel of the Fig. 7 shows the refractive index and reflectivities for the 50-50 FeCr alloy. For low photon energies or frequencies (that is large wavelengths) the refractive index and the reflectivities are small. However, around photon energies around 0.4 , 0.6 and 0.8 Ry. the refractive index becomes large and the reflectivity too becomes large and the system reflects back most of the

incident radiation. We can interpret this as saying that large refractive index means that the effective speed of light in the medium becomes very small and the photon does not propagate through the solid. The system appears shiny for these frequency (wavelengths) and, as discussed earlier in our work on CuZn⁷⁶ this determines the “color” of the alloy.

IV. SUMMARY

We have used three different techniques for the calculation of the electronic structure of fully disordered Fe_xCr_{1-x} alloys : the KKR-CPA, the TB-LMTO-ASR and the PAW-SQS. Each of the methods have their own distinct approximations and the aim was to determine, for this specific alloy system, their suitability and relative accuracy. Unlike the earlier study of Cu_xZn_{1-x}⁷⁶, we find remarkable agreement in the shapes of the density of states and their energy moments for all the three techniques. The local and averaged magnetic moments are also very similar, except for the Cr local moments in the dilute Cr limit. Unfortunately, experimental data for Cr local moment in this limit was not available. The difference in the averaged magnetic moment in the dilute limit between KKR-CPA and TB-LMTO-ASR is too small to warrant comment. Neutron scattering experiments on Fe_xCr_{1-x} alloys indicate a degree of short-ranged ordering. The single site CPA cannot effectively deal with short-ranged order. We have studied the effect of short-ranged order on the density of states of Fe_{0.5}Cr_{0.5} via a generalization of the TB-LMTO-ASR. Finally we have extended the TB-LMTO-ASR to study optical conductivity, reflectivity and refractive index for the same alloy system. These studies, coupled with our earlier study of the Cu_xZn_{1-x} alloys⁷⁶, provide us with an insight into the relative merits of these approaches and allow us to choose between them for future work.

Acknowledgments

KT would like to thank the CSIR, India for financial assistance for research. The work was done under the Asia-Sweden Research Links Program titled *Theoretical and experimental investigations on magnetic alloys*. BS and OE acknowledge computational support from Swedish National Infrastructure for Computing (SNIC). AM would like to thank the Theoretical Magnetism Group of the Department of Physics, Uppsala University for hospitality during the time this work was completed. Part of the work was done with the VASP code and the Stuttgart TB-LMTO code was used as the basis of the ASR work.

- ¹ M. Kubik, B. Handke, W. Karaś, N. Spiridis, T. Ślęzak and J. Korecki, *Phys. Stat. Sol. (a)* **189**, 705 (2002).
- ² S.L. Qiu, V.L. Moruzzi and P.M. Marcus, *J. Appl. Phys.* **85**, 4839 (1999).
- ³ S.S. Brenner, M.K. Miller, and W.A. Soffa, *Scr. Metall.* **16**, 831 (1982).
- ⁴ L.V. Curvich, I.V. Veits, V.A. Medvedev, G.A. Bergman, and V.S. Yungnan, *Thermodynamic Properties of Individual Substances.*, Vol. 4, part I, (Nauka, Moscow) 9 (1982).
- ⁵ S. Hertzman and B. Sundman, *Calphad* **6**, 67 (1982).
- ⁶ Y. Iguchi, S. Nobori, K. Saito, and T. Fuwa, *Tetsu-to-Hagane* **68**, 633 (1982).
- ⁷ R. M. Vilar and G. Cizeron, *Mem. Etud. Sci. Rev. Metall.* **79**, 687 (1982) ; *J. Mat. Sci. Lett.* **2**, 283 (1983).
- ⁸ G.I. Batalin, V.P. Kurach, and V.S. Sudavtseva, *Russ. J. Phys. Chem.* **58**, 289 (1984).
- ⁹ T. De Nys and P.M. Gielen, *Metall. Trans.* **2**, 1423 (1971).
- ¹⁰ G. Kirchner, T. Nishizawa, and B. Uhrenius, *Metall. Trans.* **4**, 167 (1973).
- ¹¹ F.N. Mazandarany and R.D. Pehlke, *Metall. Trans.* **4**, 2067 (1973).
- ¹² R.O. Williams, *Metall. Trans.* **5**, 967 (1974).
- ¹³ S. Langer, M. Bar-on, and H.D. Miller, *Phys. Rev. A* **11**, 1417 (1975).
- ¹⁴ T.I. Babynk, G.P. Kushta, and S.A. Chomey, *Phys. Met. Metallogr.* **35**(4), 176 (1973).
- ¹⁵ T.I. Babynk, G.P. Kushta, and O.I. Rybailo, *Izv. V U.Z. Chernaya Metall.* **7**, 126 (1974).
- ¹⁶ S. Katarro and M. Iizumi, *J. Phys. Soc. Jpn.* **2**, 347 (1982).
- ¹⁷ T.L. Swan-Wood, O. Delaire and B. Fultz, *Phys. Rev. B* **72**, 024305 (2005).
- ¹⁸ D. Chandra and L.H. Schwartz, *Met. Trans.* **2**, 511 (1971).
- ¹⁹ B.D. Dunlap, A.T. Aldred, R.J. Nemanich and C.W. Kimball, *AIP Conf. Proc.* **29**, 232 (1976).
- ²⁰ V.A. Makarov, I.N. Puzev, A.N. Koropiy, and T.V. Sakharova, *Phys. Met. Metallogr.* **54**, 66 (1982).
- ²¹ S.M. Dubiel and G. Inden, *Z. Metallkd.* **78**, 544 (1987).
- ²² J. Cieślak, M. Reissner, W. Steiner and S.M. Dubiel, *J. Magn. Magn. Mat.* **272-276**, 534 (2003).
- ²³ D.B. Downie and J.F. Martin, *J. Chem. Thermodyn.* **16**, 743 (1984).
- ²⁴ V.M. Polovov, *Sov. Phys. JETP*, **39**, 1064-1071 (1974).
- ²⁵ W.M. Maclnnes and K. Schröder, *Proc. Conf. Dynamical Aspects of Critical Phenomena*, 305 (1972).
- ²⁶ S. Araj and E.E. Anderson, *Physica* **54**, 617 (1971).
- ²⁷ J.C. Matthews and N. Morton, *Proc. Phys. Soc.* **85**, 343 (1965).
- ²⁸ S.K. Burke and B.D. Rainford, *J. Phys. F : Metal Phys.* **13**, 441 (1983).
- ²⁹ S.K. Burke, R. Cywinski, J.R. Davis, and B.D. Rainford, *J. Phys. F : Metal Phys.* **13**, 451 (1983).
- ³⁰ S.K. Burke and B.D. Rainford, *J. Phys. F : Metal Phys.* **13**, 471 (1983).
- ³¹ Yu.A. Dorofeyev, A.Z. Men'shikov, and G.A. Takzey, *Phys. Met. Metallogr.* **55**, 102 (1983).
- ³² A..C. Palumbo, R.D. Parks, and Y. Yeshurun, *J. Magn. Magn. Mat.* **36**, 66 (1983).
- ³³ A.T. Aldred and J.S. Kouvel, *Physica B* **86-88**, 5 (1985).
- ³⁴ V.I. Gomankov, A.I. Zaitsev, I.M. Puzev and B.N. Tretyakov, *Sov. Phys. JETP* **68**, 1462 (1988).
- ³⁵ A.I. Kordyr, A. Borisnyk, and S.A. Yur'ev, *Phys. Met. Metallogr.* **69**, 128 (1990).
- ³⁶ P.A. Beck, *Phys. Rev. B* **44**, 7115 (1991).
- ³⁷ M. Murugesan, S. Chikazawa and H. Kuwano, *Magnetism Conference, IEEE International, HC04* (1999).
- ³⁸ S.F. Fischer, S.N. Kaul and H. Kronmüller, *J. Magn. Magn. Mat.* **226-230**, 540 (2001).
- ³⁹ A.T. Aldred, *Phys. Rev. B* **14**, 216 (1976).
- ⁴⁰ C.H. Shull and M.K. Wilkinson, *Phys. Rev.* **97**, 304 (1955).
- ⁴¹ J. Cieślak, M. Reisser, W. Steiner and S.M. Dubiel, *J. Magn. Magn. Mat.* **272-276**, 534 (534).
- ⁴² C.T. Wei and C.H. Cheng, *Phys. Rev.* **124**, 722 (1961).
- ⁴³ M.M. Newman and W.H. Stevens, *Proc. Roy. Soc.* **74**, 290 (1959).
- ⁴⁴ M.V. Rao and W.A. Tiller, *Mater. Sci. Eng.* **14**, 47 (1974).
- ⁴⁵ J.-O. Andersson and B. Sundman, *Calphad* **11**, 83 (1987).
- ⁴⁶ Y.-Y. Chuang, J.-C. Lin and Y.A. Chang, *Calphad* **11**, 57 (1987).
- ⁴⁷ M.V. Rao and A. Tiller, *Scr. Metall* **6**, 417 (1972).
- ⁴⁸ S. Katano and M. Iizumi, *Physica B* **120**, 392 (1983).
- ⁴⁹ H. Kuwano, *Jpn. Int. Met.* **26**, 473 (1985).
- ⁵⁰ M. Furusaka, Y. Ishikawa and M. Mera, *Phys. Rev. Lett.* **54**, 2611 (1985).
- ⁵¹ G.I. Batalev, V.P. Kurach and V.S. Sudavtseva, *Russ. J. Phys. Chem.* **58**, 289 (1984).
- ⁵² V.L. Moruzzi, P.M. Marcus and P.C. Pattnaik, *Phys. Rev. B* **37**, 8003 (1988).
- ⁵³ V.L. Moruzzi and P.M. Marcus, *Phys. Rev. B* **42**, 8361 (1990) ; *Phys. Rev. B* **46**, 14198 (1992).
- ⁵⁴ E.G. Moroni and T. Jarlborg, *Phys. Rev. B* **47**, 3255 (1993).
- ⁵⁵ D.J. Singh, *J. Appl. Phys.* **75**, 6688 (1994).
- ⁵⁶ M.H.F. Sluiter, K. Esfarjani and Y. Kawazoe, *Phys. Rev. Lett.* **75**, 3142 (1995).
- ⁵⁷ G. Moriatis, M.A. Khan, H. Dreysee and C. Demangeat, *J. Magn. Magn. Mat.* **156**, 250 (1996).
- ⁵⁸ W.H. Butler, X. Zhang and J.M. MacLaren, *MMM-Intermaq Conference*, 301 (1998).
- ⁵⁹ P.H. Dederichs, R. Zeler, H. Akai and H. Ebert, *J. Magn. Magn. Mat.* **100**, 247 (1991).
- ⁶⁰ N.I. Kulikov and C. Demangeat, *Phys. Rev. B* **55**, 3533 (1997).
- ⁶¹ C. Jiang, C. Wolverton, J. Sofo, L. -Q. Chen and Z. -K. Liu, *Phys. Rev. B* **69** 214202 (2004).
- ⁶² A. Zunger, S. -H. Wei, L.G. Ferreira and J. E. Bernard, *Phys. Rev. Lett.* **65** 353 (1990).
- ⁶³ P. Olsson, I. A. Abrikosov and J. Wallenius, *Phys. Rev. B* **73**, 104416 (2006).
- ⁶⁴ M. Jarrell and H. R. Krishnamurthy, *Phys. Rev. B* **63**, 125102 (2001).
- ⁶⁵ D.A. Rowlands, J.B. Staunton, B. L. Gyorffy, E. Bruno and B. Ginatempo, *Phys. Rev. B* **72**, 045101 (2005).
- ⁶⁶ P.E.A. Turchi, L. Reinhard and G.M. Stocks, *Phys. Rev. B* **50**, 15542 (1994).
- ⁶⁷ A. Mookerjee in *Electronic structure of alloys, surfaces and clusters* (Tayler-Francis,UK) ed. D.D. Sarma and A. Mookerjee (2003).
- ⁶⁸ F. Liot, S. I. Simak and I. A. Abrikosov, *J. Appl. Phys.* **99**, 08P906 (2006); A. V. Ruban, S. I. Simak, S. Shallcross, and H. L. Skriver, *Phys. Rev. B* **67**, 214302 (2003).
- ⁶⁹ S. Ghosh, P.L. Leath and M.H. Cohen, *Phys. Rev. B* **66**,

- 214206 (2002).
- ⁷⁰ A. Chakrabarti and A. Mookerjee, *E. Phys. J.* **B44** 21, (2005).
- ⁷¹ A complex function $f(z)$ is called *Herglotz* if (a) its singularities lie on the real z axis (b) $\text{Sgn}(\text{Im}f(z)) = -\text{Sgn}(\text{Im}z)$ and (c) $f(z) \sim 1/z$ as $z \rightarrow \pm\infty + i0$.
- ⁷² S. Ghosh, B. Sanyal, C. Basu Chaudhuri and A. Mookerjee, *Eur. Phys. J B* **23**, 455 (2001).
- ⁷³ J. Kudrnovský and V. Drchal, *Phys. Rev. B* **41** 7515 (1990).
- ⁷⁴ D. Paudyal, T. Saha-Dasgupta and A. Mookerjee, *J. Phys. : Condens. Matter* **16**, 2317 (2004).
- ⁷⁵ A.V. Ruban and H. L. Skriver, *Phys. Rev. B* **66**, 024201 (2003).
- ⁷⁶ K. Tarafder, A.Chakrabarti, K.K. Saha and A. Mookerjee, *Phys. Rev. B* **74**, 144204 (2006).
- ⁷⁷ G. Kresse and J. Hafner, *Phys. Rev. B* **48**, 13115 (1993); G. Kresse and J. Furthmuller, *Comput. Mater. Sci.* **6**, 15 (1996).
- ⁷⁸ R. Haydock in *Lecture Notes in Physics* **35** (Academic Press).
- ⁷⁹ D. Thouless, *Phys. Rep.* **13**, 93 (1974).
- ⁸⁰ R. Elliot, *Structures of Binary Alloys* (Metallurgiya, Moscow) (1970).
- ⁸¹ A. Mookerjee and R. Prasad, *Phys. Rev. B* **48**, 17724 (1993).
- ⁸² T. Saha, I. Dasgupta and A. Mookerjee, *Phys. Rev. B* **50**, 13267 (1994).
- ⁸³ T. Saha, I. Dasgupta and A. Mookerjee, *J. Phys. : Condens. Matter* **8**, 1979 (1996).
- ⁸⁴ K.K. Saha, A. Mookerjee and O.Jepsen, *Phys. Rev. B* **71**, 094207 (2005).
- ⁸⁵ M. Fallot, *Ann. Phys. (Paris)* **6**, 305 (1936).
- ⁸⁶ H. Hasegawa and J. Kanamori, *J. Phys. Soc. Jpn.* **33**, 1607 (1972).
- ⁸⁷ G. Frolliani, F. Menzinger and F. Satchetti, *Phys. Rev. B* **11**, 2030 (1975).
- ⁸⁸ M. E. De Morton, *Phys. Rev. Lett.* **10**, 208 (1963).
- ⁸⁹ D. Paudyal, T. Saha-Dasgupta and A. Mookerjee, *J. Phys. Condens. Mat.* **16**, 2317 (2004).
- ⁹⁰ A.I. Liechtenstein, M.I. Katsnelson, V.P. Antropov and V.A. Gubanov, *J. Magn. Magn. Mat.* **67**, 65 (1987).
- ⁹¹ K. Binder, D.P. Landau and A.M. Ferrenberg, *Phys. Rev. Lett.* **74**, 298 (1995).
- ⁹² K. Tarafder and A. Mookerjee, *J. Phys. Condens. Mat.* **17**, 6435 (2005).
- ⁹³ V.S. Viswanath and G. Müller, (1993) in “*The user friendly recursion method*”, (Troisieme Cycle de la Physique, en Suisse Romande).
- ⁹⁴ A. Mookerjee, *J. Phys. C: Solid State Phys.* **6**, 1340 (1973).